



HAL
open science

Soil metabolomics: A powerful tool for predicting and specifying pesticide sorption

Jeanne Dollinger, Pierre Pétriacq, Amélie Flandin, Anatja Samouelian

► To cite this version:

Jeanne Dollinger, Pierre Pétriacq, Amélie Flandin, Anatja Samouelian. Soil metabolomics: A powerful tool for predicting and specifying pesticide sorption. *Chemosphere*, 2023, 337, pp.139302. 10.1016/j.chemosphere.2023.139302 . hal-04167438

HAL Id: hal-04167438

<https://hal.inrae.fr/hal-04167438>

Submitted on 7 Sep 2023

HAL is a multi-disciplinary open access archive for the deposit and dissemination of scientific research documents, whether they are published or not. The documents may come from teaching and research institutions in France or abroad, or from public or private research centers.

L'archive ouverte pluridisciplinaire **HAL**, est destinée au dépôt et à la diffusion de documents scientifiques de niveau recherche, publiés ou non, émanant des établissements d'enseignement et de recherche français ou étrangers, des laboratoires publics ou privés.



Distributed under a Creative Commons Attribution - NonCommercial - NoDerivatives 4.0 International License

Soil metabolomics: a powerful tool for predicting and specifying pesticide sorption

Jeanne Dollinger^{*1}, Pierre Pétriacq^{2,3}, Amélie Flandin^{2,3}, Anatja Samouelian¹

(1): UMR LISAH, Université Montpellier, INRAE, IRD, Institut Agro, 34060 Montpellier, France

(2): Univ. Bordeaux, INRAE, UMR1332 BFP, 33882 Villenave d'Ornon, France

(3): Bordeaux Metabolome, MetaboHUB, PHENOME-EMPHASIS, 33140 Villenave d'Ornon, France

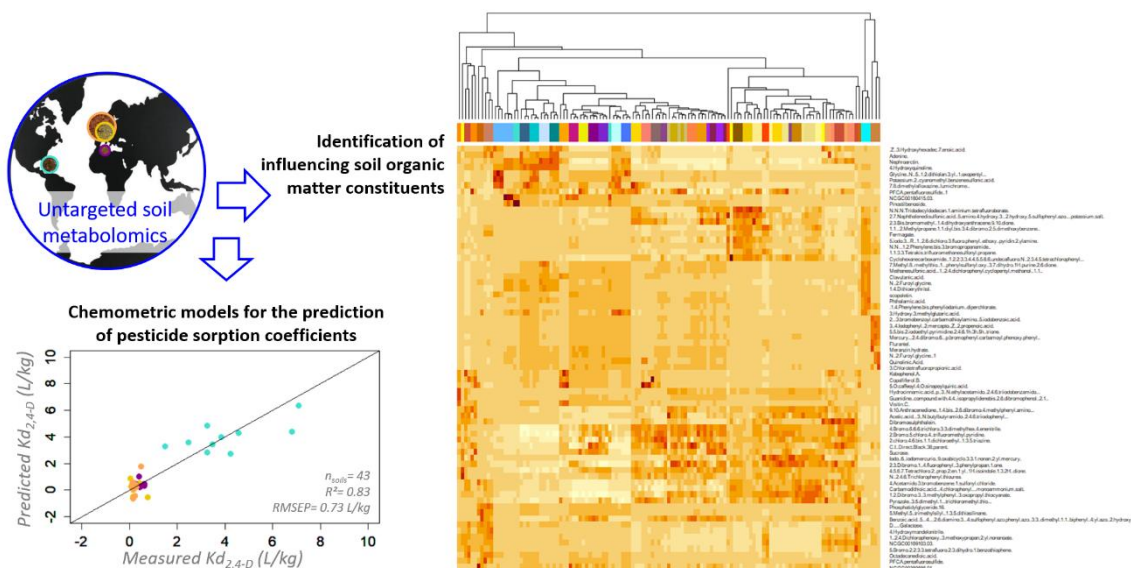
(*) corresponding author: jeanne.dollinger@inrae.fr

Abstract:

Sorption regulates the dispersion of pesticides from cropped areas to surrounding water bodies as well as their persistence. Assessing the risk of water contamination and evaluating the efficiency of mitigation measures, requires fine-resolution sorption data and a good knowledge of its drivers. This study aimed to assess the potential of a new approach combining chemometric and soil metabolomics to estimate the adsorption and desorption coefficients of a range of pesticides. It also aims to identify and characterize key components of soil organic matter (SOM) driving the sorption of these pesticides. We constituted a dataset of 43 soils from Tunisia, France and Guadeloupe (West Indies), covering extensive ranges of texture, organic carbon and pH. We performed untargeted soil metabolomics by liquid chromatography coupled with high-resolution mass spectrometry (UPLC-HRMS). We measured the adsorption and desorption coefficients of three pesticides namely glyphosate, 2,4-D and difenoconazole for these soils. We developed Partial Least Square Regression (PLSR) models for the prediction of the sorption coefficients from the RT-m/z matrix and conducted further ANOVA analyses to identify, annotate and characterise the most significant constituents of SOM in the PLSR models. The curated metabolomics matrix yielded 1213 metabolic markers. The prediction performance of the PLSR models was generally high for the adsorption coefficients $K_{d_{ads}}$ ($0.3 < R^2 < 0.8$) and for the desorption coefficients $K_{f_{des}}$ ($0.6 < R^2 < 0.8$) but low for n_{des} ($0.03 < R^2 < 0.3$). The most significant features in the predictive models were annotated with a confidence level of 2 or 3. The molecular descriptors of these putative compounds suggest that the pool of SOM compounds driving glyphosate sorption is reduced compared to 2,4-D and difenoconazole, and these compounds are generally more polar. This approach can provide estimates of the adsorption and desorption coefficients of pesticides, including polar pesticide, for contrasted pedoclimates.

Keywords: *Metabolomics; PLSR; UPLC-HRMS; Soil organic matter; Pesticide; Sorption coefficient.*

32 **Graphical abstract:**



33

34

35 **Highlights**

- 36 • We used soil metabolomics to predict and specify sorption for a range of pesticides
- 37 • Prediction performance of $K_{d_{ads}}$ and $K_{f_{des}}$ from soil metabolomics was good
- 38 • Prediction performance was lower for glyphosate than for 2,4-D and difenoconazole
- 39 • The pool of SOM compounds driving glyphosate sorption is reduced and more polar

40

41

42 **Introduction**

43 Over three million tons of synthetic pesticides are spread annually in the world to protect crops from
44 pests and weeds (Sharma et al., 2019). This extensive use of pesticides in agriculture threatens the
45 health of terrestrial and freshwater ecosystems worldwide (Sharma et al., 2019; Tang et al., 2021).
46 Their persistence and offsite transport from agricultural plots to surrounding ecosystems have
47 generated globalised contamination of surface and groundwater bodies used, among other anthropic
48 usages, for drinking water production (Malla et al., 2021; Pietrzak et al., 2019; Sharma et al., 2019).
49 Agricultural policies in several regions of the world tend to promote mitigation measures such as
50 implementing buffer zones, innovating farming technics or restricted spraying areas near vulnerable
51 drinking water wells (Farenhorst, 2006; Reichenberger et al., 2007; Srivastav, 2020). Assessing the
52 risk of water contamination by pesticides and evaluating the efficiency of mitigation measures,

53 requires implementing modelling approaches at the watershed scale (Dagès et al., 2023; Farenhorst,
54 2006; Gatel et al., 2019; Mottes et al., 2014).

55 The dispersion of pesticides by runoff or leaching is regulated mainly by sorption mechanisms
56 (Farenhorst, 2006; Kookana et al., 2014; Tang et al., 2012). Sorption also influences their persistence
57 as it modulates their bioavailability to degrading microorganisms (Kookana et al., 2014). Therefore,
58 sorption coefficients are the most sensitive parameters in models simulating the fate of pesticides in
59 cropped watersheds (Farenhorst, 2006; Wauchope et al., 2002). Yet, conventional laboratory
60 methods for measuring sorption coefficients are extremely time-consuming and expensive
61 (Forouzangohar et al., 2009). The current challenge is to gain insight into the sorption mechanisms to
62 identify and design suitable mitigation measures while generating fine-resolution sorption data for
63 accurate parametrisation of the risk assessment tools (models/indicators). This requires developing
64 methodologies for both predicting and specifying sorption mechanisms for a range of pesticides and
65 pedoclimates.

66 The estimation of sorption coefficients is traditionally based on the Koc. However, a significant
67 discrepancy in Koc ranges for all pesticides, especially for polar pesticides, has been reported (PPDB,
68 2023). While soil organic carbon (SOC) is indeed a major determinant of pesticide sorption (Weber et
69 al., 2004), not only its content but also its nature determines the extent of pesticide sorption
70 (Farenhorst, 2006; Kookana et al., 2014). Soil organic matter (SOM) is actually a complex and very
71 heterogeneous mixture of thousands of molecules (Longnecker and Kujawinski, 2017). Chemometrics
72 approaches for estimating pesticide sorption coefficients based on the functional or structural
73 characterisation of SOM such as NMR or infrared spectroscopy therefore improves the prediction
74 performance (Forouzangohar et al., 2009; Kookana et al., 2014). We hypothesised that characterising
75 SOM at the molecular level with untargeted metabolomics would be a step further in the prediction
76 accuracy, especially in understanding pesticide sorption mechanisms.

77 Untargeted metabolomics enables the chemical profiling of biologically-derived molecules in a wide
78 range of organisms (plants, microorganisms, algae, etc.) and environmental compartments such as
79 soil or water (Kikuchi et al., 2018; Matich et al., 2019; Pétriacq et al., 2017; van Dam and
80 Bouwmeester, 2016). This analytical technique aims to identify a maximum number of compounds in
81 the 50-2000 Da range (Bell et al., 2022; Swenson et al., 2015). Metabolomics has been used to
82 characterise biomarkers of exposure and effect of pesticides on soil microbial communities,
83 earthworms or plants (Jones et al., 2014; Matich et al., 2019; Simpson and McKelvie, 2009). As it can
84 provide information about the metabolic activity of soil microorganisms (Bell et al., 2022; Rodríguez
85 et al., 2020), it has also been suggested to be a powerful approach to characterise pesticide

86 biodegradation along with other omic approaches (Rodríguez et al., 2020). Yet, it has never been
87 applied to predict and specify pesticide sorption mechanisms.

88 The objectives of this study were to 1) evaluate the predictive performance of a chemometric
89 approaches based on untargeted metabolomics to estimate the adsorption and desorption
90 coefficients of a range of pesticides, including polar pesticides, and 2) identify and characterise key
91 components of SOM involved in the sorption mechanisms of these pesticides.

92

93 **2. Material and Methods**

94

95 **2.1 Chemicals**

96 Three pesticides among the most used worldwide to protect a variety of crops, including cereals,
97 orchards or vineyards (Matich et al., 2019; Sharma et al., 2019) and having contrasted physico-
98 chemical properties were selected for this study. These are: glyphosate, a hydrophilic broad-
99 spectrum post-emergence herbicide (logP -6.28); 2,4-D, a hydrophilic selective post-emergence
100 herbicide (logP -0.82) and difenoconazole, a hydrophobic systemic fungicide (logP 4.36) (PPDB,
101 2023).

102 Glyphosate has a very high aqueous solubility (100 g/L) and is a zwitterion under pH 10.2 (PPDB,
103 2023). 2,4-D also has a very high aqueous solubility (24 g/L) but is negatively charged under
104 environmental pH ranges (PPDB, 2023). Difenoconazole has a low aqueous solubility (15 mg/L) and is
105 uncharged under environmental pH ranges (PPDB, 2023).

106 Non-labeled glyphosate, 2,4-D and difenoconazole were supplied by Merck and 14C-labeled
107 pesticides by ISOBIO (Fleurus, Belgium). Sodium azide, calcium chloride, methanol and
108 dichloromethane were supplied by Merck. Methyl vanillate (n° CAS 3943-74-6) was supplied by
109 Sigma Aldrich. All the chemicals used were HPLC grade.

110

111 **2.2 Origin and characterisation of the soils**

112 A set of 43 soils sampled in four locations across the world was constituted with the purpose of
113 covering an extended range of physico-chemical properties. Ten soils were sampled in Guadeloupe,
114 West Indies (WI), over a toposequence of volcanic ash soils. The climate in this area is tropical and
115 the main crops are sugar cane and banana. The other soils were collected in three sites characterised

116 by a Mediterranean climate. Six soils were sampled in the Lebna peninsula, Tunisia (TU), where crops
117 are frequently rotating from vegetables to cereals or pasture. The other soils were sampled in two
118 vineyard catchments in southern France, the Roujan and Rieutor watersheds (FR-RO and FR-RI), a
119 few kilometers apart but characterised by contrasted soils due to variations of underground rocks
120 and pedogenesis processes. Some of the TU and FR-RO soils were sampled in un-cropped areas of
121 the sites such as fallows, hedgerows, grass strips or ditches to diversify the type and content of
122 organic carbon.

123 The texture, organic carbon content (OC), $\text{pH}_{\text{H}_2\text{O}}$ and cationic exchange capacity (CEC) were measured
124 with standardised methods at the INRAE LAS laboratory (Arras, France) for both FR-RO and FR-RI soils
125 and at the Cirad US 49 laboratory (Montpellier, France) for WI and TU soils (specific habilitation for
126 analysing foreign soils). These properties are displayed in Figure 1.

127

128 **2.3 Measurement of the sorption coefficients**

129 Both adsorption and desorption isotherms were characterised for all soils. The adsorption batch test
130 procedure was designed following the OECD guidelines n°106 (OECD, 2000). ¹⁴C-labelled glyphosate,
131 2,4-D and difenoconazole were used for the experiments. The concentration of the solutions used
132 were 5, 10, 50, 100 and 1000 $\mu\text{g}/\text{L}$. All these solutions were composed of 50% labelled/non-labelled
133 pesticides. The background electrolyte was composed of 0.01M CaCl_2 plus 200 mg/L NaN_3 except for
134 glyphosate for which the background electrolyte contained only NaN_3 to avoid an artificial increase of
135 its sorption by cation bridging (Dollinger et al., 2015). The solid-to-liquid ratio for all materials was
136 1:10 (g/mL). Solid matrices were equilibrated for 24h with the pesticide in glass tubes at a shaking
137 speed of 150 rpm. The tubes were then centrifuged at 3000 rpm (1770 g) for 10 min, and the
138 supernatant was sampled and analysed by liquid scintillation (LSC). The experiments were all
139 conducted in triplicates.

140 Following the adsorption phase, a five-step desorption was performed for all soils previously
141 equilibrated with the 100 $\mu\text{g}/\text{L}$ pesticide solutions. The supernatant was removed and replaced by an
142 equivalent volume of fresh electrolyte. After 24h shaking, the tubes were centrifuged, and the
143 supernatant was sampled for LSC analysis and replaced by fresh electrolyte.

144 Both linear (Equation 1) and Freundlich (Equation 2) models were fitted to the adsorption isotherms.
145 Given the excellent linearity of the adsorption isotherms ($0.91 < n_{\text{ads}} < 1.01$), only the linear adsorption
146 coefficients K_{ads} are used for the rest of the study. However, the desorption isotherms are non-
147 linear. Therefore, the Freundlich K_{des} and n_{des} coefficients are used. The ranges of K_{ads} , K_{des} and n_{des}

148 are presented in Figure 2. The adsorption being linear, n_{des} provides an estimation of the desorption
149 hysteresis that is considered significant when $H < 0.70$ ($H = n_{des}/n_{ads}$).

$$150 \quad C_s = K_d * C_{aq} \quad (\text{Equation 1})$$

$$151 \quad C_s = K_f * C_{aq}^n \quad (\text{Equation 2})$$

152 Where C_{aq} is the concentration in the aqueous phase at equilibrium ($\mu\text{g/L}$), K_d the linear sorption
153 coefficient (L/kg), K_f ($[\mu\text{g/kg}]/[\mu\text{g/L}]^n$) and n (-) are the Freundlich coefficients and C_s the
154 concentration in the soil ($\mu\text{g/kg}$).

155

156 **2.4 Extraction and UPLC-HRMS analysis of soils**

157 Soils were air-dried to a humidity of $\approx 10\%$ and sieved at 2 mm prior to extraction. Methanol is
158 generally used as an extraction solvent for metabolomics fingerprinting of soils (Bell et al., 2022;
159 Jones et al., 2014; Swenson et al., 2015). Given their contrasted polarity, both methanol and
160 dichloromethane (DCM) were selected as extraction solvents. This aimed to enlarge the range of
161 extractible metabolites and target polar to apolar compounds likely involved in pesticide sorption
162 mechanisms. Two successive extractions with methanol and a third with dichloromethane were
163 performed. Methyl vanillate was used as an internal standard and added to the extraction solvents at
164 25 mg/L. For each soil, five grams (equivalent dry weight) were ultrasonicated for an hour with 10 mL
165 of methanol in glass tubes. The tubes were then centrifuged for 10 min at 3000 rpm (1770 g) and the
166 supernatant was collected. Successively, 30 min ultrasonication with 10 mL methanol and 15 min
167 ultrasonication with 10 mL DCM were performed. The extracts were collected, gathered, dried under
168 nitrogen flux until dryness and suspended in 3 mL methanol. The extracts were then filtered with
169 Nalgen 0.02 μm PTFE filters. Extracts were stored in HPLC amber vials in the freezer at -18°C until
170 analysis. For each soil, the extraction was performed in triplicates. Five methodological blanks were
171 processed in the same way.

172 Untargeted metabolomics of soil samples was performed by liquid chromatography coupled with
173 high-resolution mass spectrometry (UPLC-HRMS) using a protocol developed by *Bordeaux*
174 *Metabolome*, as previously described (Dussarrat et al., 2022). Briefly, we used an Ultimate 3000
175 ultra-high-pressure liquid chromatography (UHPLC) system coupled to an LTQ-Orbitrap Elite mass
176 spectrometer interfaced with an electrospray (ESI) ionisation source (ThermoScientific, Bremen,
177 Germany), controlled by Thermo XCalibur v.3.0.63 software. Chromatographic separation was
178 achieved at a flow rate of 350 $\mu\text{L}/\text{min}$ using a GEMINI UHPLC C18 column (150×2 mm, 3 μm , Le
179 Pecq, Phenomenex, France) coupled to a C18 SecurityGuard GEMINI pre-column (4×2 mm, 3 μm , Le

180 Pecq, Phenomenex, France). The column was maintained at 35 °C, and the injection volume was 5 µL.
181 The mobile phase consisted of solvent (1) (0.05% (v/v) formic acid in water) and solvent (2)
182 (acetonitrile) with the following gradient: 0–0.5 min 3% (2), 0.5–1 min 3% (2), 1–9 min 50% (2), 9–13
183 min 100% (2), 13–14 min 100% (2), 14–14.5 min 3% (2), 14.5–18 min 3% (2). Ionisation was
184 performed in negative mode with the following parameters: ESI- (Heater temp: 300 °C, Sheath Gas
185 Flow Rate: 45 (arb), Aux Gas Flow Rate: 15 (arb), Sweep Gas Flow Rate: 10 (arb), I Spray Voltage: 2.5
186 kV, Capillary Temp: 300 °C, S-Lens RF Level: 60%). Prior to analyses, the LTQ-Orbitrap was calibrated
187 by infusing a solution of the calibration (Pierce© ESI Negative Ion Calibration Solution (ref: 88324).
188 Sixteen QC samples (*i.e.* a pool of 15 µL of each sample extract) and five methodological blanks were
189 injected to correct for mass spectrometer signal drift, and to filter out variables detected in blanks,
190 respectively. MS2 Data Dependent Analysis (DDA) was performed on all samples, QC and blank
191 extracts to generate fragmentation information for further annotation with the following
192 parameters: FTMS (50 - 1500 Da) at a resolution of 60k at 200 *m/z*; activation type, CID; isolation
193 width, 1 Da; normalised collision energy, 35 eV; activation Q, 0.250; activation time, 10 ms). In
194 addition, high-resolution MS1 full scan detection of ions was performed for 3 QC samples by FTMS
195 (50 - 1500 Da) at a resolution of 240k at 200 *m/z*.

196

197 **2.5 Metabolomic workflow**

198 Raw UPLC-HRMS data were processed using MS-DIAL v 4.90 (Tsugawa et al., 2015), yielding 17 770
199 RT-*m/z* features (parameter report available as Supplementary material, Appendix A). Briefly, MS-
200 DIAL parameters were as follows: MS1, tolerance, 0.01 Da; MS2 tolerance, 0.025 Da; retention time
201 begin, 0 min; retention time end, 18 min; minimum peak height, 10 000; mass slice width, 0.05 Da;
202 smoothing filter, Linear Weighted Moving Average; smoothing level, 4 scans; minimum peak width, 5
203 scans; sigma window value, 0.5. After data-cleaning (blank check, SN > 10, CV QC < 30%), 3936
204 variables were retained for further chemometrics. MS-DIAL annotation of metabolic features was
205 performed using the online library MSMS-Public-Neg-VS16.msp with the following parameters:
206 retention time tolerance, 100 min; accurate mass tolerance (MS1), 0.01 Da; accurate mass tolerance
207 (MS2), 0.05 Da; identification score cut off, 80%. Putative annotation of differentially expressed
208 metabolites resulted from MS-DIAL screening of the MS1 detected exact HR *m/z* and MS2
209 fragmentation patterns against multiple online databases
210 (<http://prime.psc.riken.jp/compms/msdial/main.html#MSP>) (Tsugawa et al., 2015).

211 Next, manual curation of the data matrix was performed. Features present in less than three soils
212 were removed. The matrix was also screened for false positives. Therefore, features with the same

213 retention time, same m/z and that correlated significantly were considered the same compound and
214 merged. Out of the 3936 features in the curated matrix only 1213 remained after this step. The
215 values of the matrix were then centered-reduced.

216 One-way ANOVA analysis was conducted with the aov function of R (R Core Team, 2021) to identify
217 features/metabolites with peak intensities significantly varying among the soils. A heatmap of the 50
218 most discriminating features (lowest p-values) from ANOVA was constructed with R (Figure 3).
219 Features that could not be annotated with MS-DIAL were annotated with METLIN
220 (<https://metlin.scripps.edu/>) based on the MS1 exact HR m/z . The putative compounds, level of
221 confidence and adducts are displayed in Table 1.

222

223 **2.6 Chemometric prediction and specification of the pesticide sorption coefficients**

224 Partial least square regression (PLSR) was performed with the pls package of R (R Core Team, 2021)
225 to establish predictive models for K_{ads} , Kf_{des} and n_{des} of the three pesticides. The number of
226 components in the PLSR was adjusted for each predictive model with cross-validation data (lowest
227 RMSEP). The number of components varied from 4 to 9 for K_{ads} , from 5 to 25 for Kf_{des} and from 6 to
228 20 for n_{des} . Leave-one-out cross-validation was used to evaluate the performance of the predictions.
229 Both the R^2 and RMSEP values were used to evaluate the performance of the models.

230 In order to gain insight into the adsorption mechanisms, the most discriminant features were
231 selected from the PLSR. The top 20 features from the first component and the 10 top features from
232 the other components were annotated (Supplementary material tables S1 to S3). Several molecular
233 descriptors of these putative compounds, including the topological polar surface area (TPSA) (Å), the
234 H-bound donor and acceptor count and the logP were extracted from PUBCHEM (Figure 4).

235

236 **3. Results**

237 **3.1 Soil properties and pesticide sorption**

238 The set of soils selected for this study covers most of the texture classes (Fig. 1) and an extensive
239 range of SOC (0.46 – 6.50%), pH (4.63 – 8.68) and CEC (5.90 – 48.50 cmol/kg). The untargeted-
240 metabolomic analyses provide information about the nature of SOC at a molecular level. This
241 chemical profiling of SOC reveals that the extracted metabolites significantly differ in their nature
242 and relative proportions among the 43 soils. ANOVA analysis based on the relative peak intensities of
243 these metabolites enables identifying features having contrasted proportions among the studied

244 soils. The ANOVA analysis shows that out of the 1213 metabolites extracted (section 2.5), 1164 had
245 peak intensity being significantly different among the 43 soils (p -value <0.05). The heatmap of the 50
246 most significant features (lowest p -values) (Figure 3) shows that, except for four soils, the three
247 replicates were grouped under the same sub-clusters. This suggests that each soil has a distinct
248 chemical profile. The WI soils are grouped under two clusters well separated from the other soils.
249 The soils from the other sampling sites were dispatched in several sub-clusters, especially the TU
250 soils (Figure 3). Including more features in the clustering discriminated better the origin of the soils,
251 especially for the FR-RO and FR-RI soils, as displayed in the top 100 features' heatmap (Figures S1)
252 and the heatmap based on all features (data not shown).

253 Table 1 shows the annotation of the top 50 significant features. Most of these metabolites (49) could
254 be annotated with MS-DIAL or METLIN (see section 2.5) with a confidence level 2 or 3. The putative
255 annotation suggests that about 25% of these metabolites are fatty acids or other organic acids. Their
256 accurate mass range from 114 to 1018 Da and their retention time from 0.9 to 18 min suggesting a
257 large range of structure complexity and of polarity. Indeed, most of these putative compounds
258 contain aromatic moieties as well as polar functional groups. Furthermore, some of these features
259 correlated significantly with one or several other features having similar retention time, suggesting
260 they might be a fraction of a bigger molecule.

261 The adsorption and desorption coefficients of glyphosate, 2,4-D and difenoconazole covered several
262 orders of magnitude across this set of soils (Figure 2). The sorption behaviour was also contrasted
263 among the three pesticides. Glyphosate has a moderate to high adsorption ($K_{d_{ads}}$ 3.2 – 28.8 L/kg) and
264 a very strong desorption hysteresis ($K_{f_{des}}$ 263 – 4844 ($[\mu\text{g}/\text{kg}]/[\mu\text{g}/\text{L}]^n$) & n_{des} 0.03 – 0.25).
265 Difenoconazole has a very high adsorption ($K_{d_{ads}}$ 8.5 – 228.5 L/kg) and a strong desorption hysteresis
266 ($K_{f_{des}}$ 140 – 4116 ($[\mu\text{g}/\text{kg}]/[\mu\text{g}/\text{L}]^n$) & n_{des} 0.03 – 0.65). Last, exception made for the WI soils ($K_{d_{ads}}$ 1.5 –
267 7.1 L/kg, $K_{f_{des}}$ 189 – 624 ($[\mu\text{g}/\text{kg}]/[\mu\text{g}/\text{L}]^n$) & n_{des} 0.11 – 0.40), 2,4-D is weakly adsorbed ($K_{d_{ads}}$ 0.02 –
268 0.6 L/kg) and has high to no desorption hysteresis ($K_{f_{des}}$ 0 – 21 ($[\mu\text{g}/\text{kg}]/[\mu\text{g}/\text{L}]^n$) & n_{des} 0.03 – 1.55).
269 2,4-D was so weakly adsorbed on FR-RO soils and the desorption so elevate that accurate
270 measurement of $K_{f_{des}}$ and n_{des} for these soils was not possible. There was no 2,4-D left at a
271 quantifiable level after the first desorption step so the values of $K_{f_{des}}$ were set to 0 and n_{des} to 1 for
272 these FR-RO soils. The correlation of these sorption coefficients with SOC are displayed in figure S2
273 (supplementary material)

274

275 3.2 Chemometric estimation of the pesticide sorption coefficients

276 Figure 5 displays the prediction performance of the PLSR models established to predict the
277 adsorption and desorption coefficients of glyphosate, 2,4-D and difenoconazole. This performance,
278 featured by the R^2 (-) and RSMEP (L/kg) values, varies across the range of coefficients and pesticides
279 considered. The performance increase from glyphosate < difenoconazole < 2,4-D. For difenoconazole
280 and 2,4-D the prediction performance is good for $K_{d_{ads}}$ and $K_{f_{des}}$ but the regressions are driven by the
281 high values of the WI soils. It is interesting to note that the glyphosate- $K_{d_{ads}}$ PLSR has only 4
282 components while 2,4-D and difenoconazole have 8 and 9 components, respectively. This suggests
283 that the range of metabolites involved in the adsorption of glyphosate is reduced compared to 2,4-D
284 and difenoconazole.

285 The putative annotation of the most significant features in the PLSR models (highest absolute loading
286 weight (see section 2.6)) is presented in the supplementary material (Tables S1 to S3). 41 compounds
287 were annotated for glyphosate, 70 for 2,4-D and 83 for difenoconazole. It is interesting to note that
288 only one of these compounds was in these three datasets. This compound is also the only one that
289 the glyphosate and difenoconazole datasets have in common. There are six compounds commons to
290 the glyphosate and 2,4-D datasets and 22 commons to the 2,4-D and difenoconazole datasets. Few
291 compounds of the 2,4-D (4) and difenoconazole (3) datasets (Tables S2 & S3) are in the top 50
292 compounds discriminating most the SOM molecular profiles listed in Table 1.

293 Figure 4 shows the density functions of six molecular descriptors of these putatively annotated
294 datasets of compounds. Among these six descriptors only the accurate mass (m/z) and the retention
295 time (RT) are independent of the annotation. The TPSA, the H-bound donor and acceptor counts and
296 logP depend on the feature annotations that were achieved at the confidence levels 2-3. In general,
297 the distribution of these molecular descriptors is larger for difenoconazole than for glyphosate and
298 2,4-D has intermediate distribution patterns. It is interesting to note that the putative metabolites
299 with the highest TPSA ($\approx 500 \text{ \AA}$) are found only in the glyphosate dataset that also have a greater
300 proportion of compounds in the 100-200 \AA TPSA range compared to the 2,4-D and difenoconazole
301 datasets. There is also an occurrence of compounds with very low logP in the glyphosate dataset that
302 is not observed in the two other datasets. Last, there is a lower proportion of compounds with high
303 RT (10-18 min) in the glyphosate dataset. This suggests that the pool of metabolite involved in the
304 adsorption of glyphosate is more polar than those involved in the adsorption of 2,4-D and
305 difenoconazole.

306

307 4. Discussion

308 The adsorption and desorption coefficients measured for the three selected pesticides cover a range
309 of several orders of magnitude (Figure 2). This was expected from the great variability of physico-
310 chemical properties of the 43 sampled soils (Figure 1).

311 For 2,4-D and difenoconazole, the measured $K_{d_{ads}}$ values cover the entire ranges of K_d reported in
312 the literature (Akyol et al., 2021; Godeau et al., 2021; Gurson et al., 2019; PPDB, 2023; Wang et al.,
313 2020; Werner et al., 2013). The $K_{d_{ads}}$ values of glyphosate are in the low-medium range of values
314 reported in the literature (Akyol et al., 2021; Dollinger et al., 2015; Gurson et al., 2019). However,
315 higher K_d values reported for glyphosate were measured with $CaCl_2$ as background electrolyte which
316 significantly and artificially increases the K_d values (Cruz et al., 2007; de Jonge and Wollesen de
317 Jonge, 1999; Dollinger et al., 2015). These extended $K_{d_{ads}}$ ranges are ideal for testing the global
318 performance of the chemometric estimation approach based on soil metabolomic profiles. However,
319 its site-specific performance, which is the scale targeted by the risk assessment modelling, should be
320 further evaluated.

321 Desorption data are usually scarce in the literature and the desorption hysteresis is actually not
322 represented in the pesticide fate models. The $K_{f_{des}}$ and n_{des} coefficients show that the desorption
323 hysteresis is very strong for glyphosate and difenoconazole. It is also relatively strong for 2,4-D on the
324 WI soils (Figure 2). While these coefficients cannot be implemented in the models, they help evaluate
325 the uncertainty of model outputs.

326 The PLSR performance criteria (R^2 & RMSEP) indicate that for the three pesticides, the metabolomic
327 profile explains, in part, the variability of the $K_{d_{ads}}$ and $K_{f_{des}}$ (Figure 5). N_{des} seems to be less
328 influenced by the chemical characteristics of SOM (Figure 5). The prediction performance of the PLSR
329 models is lower for the glyphosate sorption coefficients than for those of 2,4-D and difenoconazole.
330 However, for 2,4-D and difenoconazole, the PLSR are forced by the high WI values which questions
331 the site-specific performance for the other sampling sites. For the three pesticides the coefficient of
332 variation of the $K_{d_{ads}}$ measures is 7-8% (calculated from the batch replicates see section 2.3). For the
333 average $K_{d_{ads}}$ values, it represents a disparity of 1.4 L/kg for glyphosate, 3.8 L/kg for difenoconazole
334 and 0.09 L/kg for 2,4-D. The RMSEP are 3 to 8 times higher than these experimental uncertainties but
335 are quite low compared to the $K_{d_{ads}}$ ranges (Figure 5).

336 The three pesticides selected for this study cover an extended range of polarity. Glyphosate
337 comprises only polar functional groups and difenoconazole only hydrophobic groups, while 2,4-D
338 contains both polar and hydrophobic moieties. The presence of polar functional groups in the
339 pesticide structure tends to diversify the type of interaction between the pesticide and the soils
340 compared to hydrophobic pesticides (Dollinger et al., 2015; Weber et al., 2004; Werner et al., 2013).

341 The adsorption coefficients of polar pesticides are generally significantly correlated to the SOM
342 content (Akyol et al., 2021; Gurson et al., 2019; Weber et al., 2004), but also to other soil
343 constituents, such as clay minerals (Dollinger et al., 2015; Weber et al., 2004). They are also very
344 sensitive to soil pH, which dictates their speciation and the surface charges of edaphic constituents
345 (Boivin et al., 2005; Kah and Brown, 2007; Wauchope et al., 2002; Weber et al., 2004).

346 In particular, the adsorption of glyphosate was reported to be driven chiefly by clay minerals and
347 metal oxides with a strong influence of pH and CEC (Dollinger et al., 2015). Some studies highlighted
348 that the sorption of glyphosate was also strongly influenced by SOM (Akyol et al., 2021; Gurson et al.,
349 2019). However, for the set of studied soils, the influence of SOM was weak (Figure S2). This explains
350 the low performance of the chemometric approach for estimating the adsorption and desorption
351 coefficients of glyphosate from the SOM metabolite profile (Figure 5). Yet the correlations are
352 significant and the RMSEP are lower than for traditional estimation approaches like pedotransfer
353 functions (Dollinger et al., 2015). The number of components in the PLSR models (Figure 5) suggests
354 that the pool of SOM compounds involved in the sorption of glyphosate is low compared to 2,4-D
355 and difenoconazole. The distribution of the molecular descriptors (Figure 4) indicates that these are
356 also more polar. However, the molecular descriptors depend on the annotation that was achieved at
357 confidence levels 2-3 (Blaženović et al., 2018; Chaleckis et al., 2019; Creek et al., 2014).

358 The metabolomics profile is highly depends on the soil extraction procedure (Bell et al., 2022;
359 Chaleckis et al., 2019; Swenson et al., 2015). Water was not used as an extraction solvent to avoid
360 the extraction of small and very polar metabolites that constitute most of the dissolved organic
361 matter fraction (DOM) (Swenson et al., 2015). Indeed, DOM has a complex and ambiguous role in the
362 sorption of pesticides (Barriuso et al., 2011) that falls behind the scope of this study. With methanol
363 and dichloromethane we targeted larger and less polar compounds. Accurate annotation of the
364 extracted compounds is still the major bottleneck of un-targeted metabolomics (Bell et al., 2022;
365 Blaženović et al., 2018; Chaleckis et al., 2019). The potential of metabolomics is huge to specify the
366 mechanism involved in the fate of pesticides in soils including sorption and degradation (Rodrigues et
367 al., 2013). However, further specification of these mechanisms would require the identification of
368 metabolites with a confidence level of 1 or 2. This therefore points to the lack of representation of
369 soil compounds in metabolomic databases (Pétriacq et al., 2017).

370 The metabolomic profiling procedure seems relatively stable, as displayed by the clustering of the
371 replicates for 90% of the soils (Figure 3). For the present study, all extracts were injected in the same
372 LC run. UPLC-HRMS analysis is subjected to retention time shifts which hinders the performance of
373 the peak alignment if the extracts are not injected in the same run. Another limit to the number of

374 extracts that can be processed is the multiplication of the detected features. Indeed, multiplying the
375 extracts increases the risk of noise in the matrix (*i.e.* features present in less than 5-10% of the
376 samples). The curation of the metabolomics matrix to remove this noise is time-consuming.

377

378 **Conclusion**

379 Chemometrics based on metabolomics data is a powerful approach to predict the pesticide
380 adsorption and desorption coefficients for soils having contrasted physico-chemical properties. The
381 prediction performance is lower for glyphosate than for 2,4-D and difenoconazole but higher than for
382 traditional pedotransfer functions. The establishment of the PLSR models is time-consuming. Yet
383 once this is achieved, a single extract can provide estimations for both adsorption and desorption
384 coefficients for the whole range of pesticides tested. Therefore, it is beneficial to diversify the range
385 of pesticides included in the risk assessment modelling. It can also help to refine the resolution of the
386 sorption parametrisation in the models. The approach was tested for a very diverse set of soils, but
387 its site-specific precision remains to be evaluated. It might not be the most rapid and precise
388 estimation methods for the spatialisation of sorption coefficients. However, metabolomics is also a
389 potential indicator of other mechanisms involved in the fate of pesticides, including biodegradation.
390 Its ability to provide information on the biodegradation of pesticides, their presence and their effect
391 on the environment should be further investigated to develop a global estimation approach.
392 Metabolomics also help to gain insight into the sorption mechanisms and the fraction of SOM
393 involved. The spectra databases' development should help improve the accuracy of the metabolite
394 annotation.

395

396 **Acknowledgement**

397 The authors would like to thank David Fages and Olivier Grünberger for their help with the soil
398 sampling. We also thank Sandrine Negro and Manon Lagacherie for their help with the measurement
399 of the sorption coefficients. Last we warmly thank Pauline Campan for providing the sorption
400 coefficients and soil physico-chemical properties of the WI soils.

401

402 **Statements & Declarations**

403 **Availability of data and materials**

404 The datasets used and/or analysed during the current study are available from the corresponding
405 author upon reasonable request.

406 **Competing interests**

407 The authors declare that they have no known competing financial interests or personal relationships
408 that could have appeared to influence the work reported in this paper.

409 **Authors' contributions**

410 Jeanne Dollinger contributed a vast majority of the study conception and design with the help of
411 Anatja Samouelian and Pierre Pétriacq. Jeanne Dollinger performed the soil extractions and the
412 measurement of the sorption coefficients for the FR-RO, FR-RI & TU soils. Data on the WI soils were
413 provided by Anatja Samouelian. UPLC-HRMS-based metabolomics was performed by Pierre Pétriacq
414 and Amelie Flandin. The first draft of the manuscript was written by Jeanne Dollinger, and all authors
415 commented on previous versions of the manuscript. All authors read and approved the final
416 manuscript.

417 **Funding**

418 The study was funded by a young scientist starting grant from the AgroEcoSystem department of
419 INRAE. The authors are grateful for financial support from MetaboHUB (ANR-11-INBS-0010).

420 **Ethical Approval**

421 Not applicable

422 **Consent to Participate**

423 Not applicable

424 **Consent to Publish**

425 Not applicable

426

427 **References**

- 428 Akyol, N.H., Carroll, K.C., Ciftci Cortuk, E., Gunduz, O.C., Sahin, N., 2021. Comparison of sorption and
429 solute transport behaviour of several herbicides in an alkaline agricultural soil. *Int. J. Environ.*
430 *Anal. Chem.* 0, 1–19. <https://doi.org/10.1080/03067319.2021.1969384>
- 431 Barriuso, E., Andrades, M.-S., Benoit, P., Houot, S., 2011. Pesticide desorption from soils facilitated by
432 dissolved organic matter coming from composts: experimental data and modelling approach.
433 *Biogeochemistry* 106, 117–133. <https://doi.org/10.1007/s10533-010-9481-y>
- 434 Bell, M.A., McKim, U., Sproule, A., Tobalt, R., Gregorich, E., Overy, D.P., 2022. Extraction methods for
435 untargeted metabolomics influence enzymatic activity in diverse soils. *Sci. Total Environ.* 828,
436 154433. <https://doi.org/10.1016/j.scitotenv.2022.154433>

437 Blaženović, I., Kind, T., Ji, J., Fiehn, O., 2018. Software Tools and Approaches for Compound
438 Identification of LC-MS/MS Data in Metabolomics. *Metabolites* 8, 31.
439 <https://doi.org/10.3390/metabo8020031>

440 Boivin, A., Cherrier, R., Schiavon, M., 2005. A comparison of five pesticides adsorption and desorption
441 processes in thirteen contrasting field soils. *Chemosphere* 61, 668–676.
442 <https://doi.org/10.1016/j.chemosphere.2005.03.024>

443 Chaleckis, R., Meister, I., Zhang, P., Wheelock, C.E., 2019. Challenges, progress and promises of
444 metabolite annotation for LC–MS-based metabolomics. *Curr. Opin. Biotechnol., Analytical*
445 *Biotechnology* 55, 44–50. <https://doi.org/10.1016/j.copbio.2018.07.010>

446 Creek, D.J., Dunn, W.B., Fiehn, O., Griffin, J.L., Hall, R.D., Lei, Z., Mistrik, R., Neumann, S., Schymanski,
447 E.L., Sumner, L.W., Trengove, R., Wolfender, J.-L., 2014. Metabolite identification: are you
448 sure? And how do your peers gauge your confidence? *Metabolomics* 10, 350–353.
449 <https://doi.org/10.1007/s11306-014-0656-8>

450 Cruz, L.H. da, Santana, H. de, Zaia, C.T.B.V., Zaia, D.A.M., 2007. Adsorption of glyphosate on clays and
451 soils from Paraná State: effect of pH and competitive adsorption of phosphate. *Braz. Arch.*
452 *Biol. Technol.* 50, 385–394. <https://doi.org/10.1590/S1516-89132007000300004>

453 Dagès, C., Voltz, M., Bailly, J.-S., Crevoisier, D., Dollinger, J., Margoum, C., 2023. PITCH: A model
454 simulating the transfer and retention of pesticides in infiltrating ditches and channel
455 networks for management design purposes. *Sci. Total Environ.* 891, 164602.
456 <https://doi.org/10.1016/j.scitotenv.2023.164602>

457 de Jonge, H., Wollesen de Jonge, L., 1999. Influence of pH and solution composition on the sorption
458 of glyphosate and prochloraz to a sandy loam soil. *Chemosphere* 39, 753–763.
459 [https://doi.org/10.1016/S0045-6535\(99\)00011-9](https://doi.org/10.1016/S0045-6535(99)00011-9)

460 Dollinger, J., Dagès, C., Voltz, M., 2015. Glyphosate sorption to soils and sediments predicted by
461 pedotransfer functions. *Environ. Chem. Lett.* 13, 293–307. [https://doi.org/10.1007/s10311-](https://doi.org/10.1007/s10311-015-0515-5)
462 [015-0515-5](https://doi.org/10.1007/s10311-015-0515-5)

463 Dussarrat, T., Prigent, S., Latorre, C., Bernillon, S., Flandin, A., Díaz, F.P., Cassan, C., Van Delft, P.,
464 Jacob, D., Varala, K., Joubes, J., Gibon, Y., Rolin, D., Gutiérrez, R.A., Pétriacq, P., 2022.
465 Predictive metabolomics of multiple Atacama plant species unveils a core set of generic
466 metabolites for extreme climate resilience. *New Phytol.* 234, 1614–1628.
467 <https://doi.org/10.1111/nph.18095>

468 Farenhorst, A., 2006. Importance of Soil Organic Matter Fractions in Soil-Landscape and Regional
469 Assessments of Pesticide Sorption and Leaching in Soil. *Soil Sci. Soc. Am. J.* 70, 1005–1012.
470 <https://doi.org/10.2136/sssaj2005.0158>

471 Forouzangohar, M., Cozzolino, D., Kookana, R.S., Smernik, R.J., Forrester, S.T., Chittleborough, D.J.,
472 2009. Direct Comparison between Visible Near- and Mid-Infrared Spectroscopy for
473 Describing Diuron Sorption in Soils. *Environ. Sci. Technol.* 43, 4049–4055.
474 <https://doi.org/10.1021/es8029945>

475 Gatel, L., Lauvernet, C., Carluer, N., Weill, S., Tournebize, J., Paniconi, C., 2019. Global evaluation and
476 sensitivity analysis of a physically based flow and reactive transport model on a laboratory
477 experiment. *Environ. Model. Softw.* 113, 73–83.
478 <https://doi.org/10.1016/j.envsoft.2018.12.006>

479 Godeau, C., Morin-Crini, N., Staelens, J.-N., Martel, B., Rocchi, S., Chanet, G., Fourmentin, M., Crini,
480 G., 2021. Adsorption of a triazole antifungal agent, difenoconazole, on soils from a cereal
481 farm: Protective effect of hemp felt. *Environ. Technol. Innov.* 22, 101394.
482 <https://doi.org/10.1016/j.eti.2021.101394>

483 Gurson, A.P., Ozbay, I., Ozbay, B., Akyol, G., Akyol, N.H., 2019. Mobility of 2,4-Dichlorophenoxyacetic
484 Acid, Glyphosate, and Metribuzine Herbicides in Terra Rossa-Amended Soil: Multiple
485 Approaches with Experimental and Mathematical Modeling Studies. *Water. Air. Soil Pollut.*
486 230, 220. <https://doi.org/10.1007/s11270-019-4266-y>

487 Jones, O.A.H., Sdepanian, S., Lofts, S., Svendsen, C., Spurgeon, D.J., Maguire, M.L., Griffin, J.L., 2014.
488 Metabolomic analysis of soil communities can be used for pollution assessment. *Environ.*
489 *Toxicol. Chem.* 33, 61–64. <https://doi.org/10.1002/etc.2418>
490 Kah, M., Brown, C.D., 2007. Prediction of the Adsorption of Ionizable Pesticides in Soils. *J. Agric. Food*
491 *Chem.* 55, 2312–2322. <https://doi.org/10.1021/jf063048q>
492 Kikuchi, J., Ito, K., Date, Y., 2018. Environmental metabolomics with data science for investigating
493 ecosystem homeostasis. *Prog. Nucl. Magn. Reson. Spectrosc.* 104, 56–88.
494 <https://doi.org/10.1016/j.pnmrs.2017.11.003>
495 Kookana, R.S., Ahmad, R., Farenhorst, A., 2014. Sorption of Pesticides and its Dependence on Soil
496 Properties: Chemometrics Approach for Estimating Sorption, in: *Non-First Order Degradation*
497 *and Time-Dependent Sorption of Organic Chemicals in Soil*, ACS Symposium Series. American
498 Chemical Society, pp. 221–240. <https://doi.org/10.1021/bk-2014-1174.ch012>
499 Longnecker, K., Kujawinski, E.B., 2017. Mining mass spectrometry data: Using new computational
500 tools to find novel organic compounds in complex environmental mixtures. *Org. Geochem.*
501 110, 92–99. <https://doi.org/10.1016/j.orggeochem.2017.05.008>
502 Malla, M.A., Gupta, S., Dubey, A., Kumar, A., Yadav, S., 2021. Chapter 7 - Contamination of
503 groundwater resources by pesticides, in: *Ahamad, A., Siddiqui, S.I., Singh, P. (Eds.),*
504 *Contamination of Water*. Academic Press, pp. 99–107. [https://doi.org/10.1016/B978-0-12-](https://doi.org/10.1016/B978-0-12-824058-8.00023-2)
505 [824058-8.00023-2](https://doi.org/10.1016/B978-0-12-824058-8.00023-2)
506 Matich, E.K., Chavez Soria, N.G., Aga, D.S., Atilla-Gokcumen, G.E., 2019. Applications of metabolomics
507 in assessing ecological effects of emerging contaminants and pollutants on plants. *J. Hazard.*
508 *Mater.* 373, 527–535. <https://doi.org/10.1016/j.jhazmat.2019.02.084>
509 Mottes, C., Lesueur-Jannoyer, M., Le Bail, M., Malézieux, E., 2014. Pesticide transfer models in crop
510 and watershed systems: a review. *Agron. Sustain. Dev.* 34, 229–250.
511 <https://doi.org/10.1007/s13593-013-0176-3>
512 OECD, 2000. Test No. 106: Adsorption -- Desorption Using a Batch Equilibrium Method. Organisation
513 for Economic Co-operation and Development, Paris.
514 Pétriacq, P., Williams, A., Cotton, A., McFarlane, A.E., Rolfe, S.A., Ton, J., 2017. Metabolite profiling of
515 non-sterile rhizosphere soil. *Plant J.* 92, 147–162. <https://doi.org/10.1111/tpj.13639>
516 Pietrzak, D., Kania, J., Malina, G., Kmiecik, E., Wątor, K., 2019. Pesticides from the EU First and Second
517 Watch Lists in the Water Environment. *CLEAN – Soil Air Water* 47, 1800376.
518 <https://doi.org/10.1002/clen.201800376>
519 PPDB, 2023. Pesticide Properties Database [WWW Document]. URL
520 <http://sitem.herts.ac.uk/aeru/ppdb/en/search.htm> (accessed 1.6.23).
521 R Core Team, 2021. R: A Language and Environment for Statistical Computing.
522 Reichenberger, S., Bach, M., Skitschak, A., Frede, H.-G., 2007. Mitigation strategies to reduce
523 pesticide inputs into ground- and surface water and their effectiveness; A review. *Sci. Total*
524 *Environ.* 384, 1–35. <https://doi.org/10.1016/j.scitotenv.2007.04.046>
525 Rodrigues, E.T., Lopes, I., Pardal, M.Â., 2013. Occurrence, fate and effects of azoxystrobin in aquatic
526 ecosystems: A review. *Environ. Int.* 53, 18–28. <https://doi.org/10.1016/j.envint.2012.12.005>
527 Rodríguez, A., Castrejón-Godínez, M.L., Salazar-Bustamante, E., Gama-Martínez, Y., Sánchez-Salinas,
528 E., Mussali-Galante, P., Tovar-Sánchez, E., Ortiz-Hernández, Ma.L., 2020. Omics Approaches
529 to Pesticide Biodegradation. *Curr. Microbiol.* 77, 545–563. [https://doi.org/10.1007/s00284-](https://doi.org/10.1007/s00284-020-01916-5)
530 [020-01916-5](https://doi.org/10.1007/s00284-020-01916-5)
531 Sharma, A., Kumar, V., Shahzad, B., Tanveer, M., Sidhu, G.P.S., Handa, N., Kohli, S.K., Yadav, P., Bali,
532 A.S., Parihar, R.D., Dar, O.I., Singh, K., Jasrotia, S., Bakshi, P., Ramakrishnan, M., Kumar, S.,
533 Bhardwaj, R., Thukral, A.K., 2019. Worldwide pesticide usage and its impacts on ecosystem.
534 *SN Appl. Sci.* 1, 1446. <https://doi.org/10.1007/s42452-019-1485-1>
535 Simpson, M.J., McKelvie, J.R., 2009. Environmental metabolomics: new insights into earthworm
536 ecotoxicity and contaminant bioavailability in soil. *Anal. Bioanal. Chem.* 394, 137–149.
537 <https://doi.org/10.1007/s00216-009-2612-4>

538 Srivastav, A.L., 2020. Chapter 6 - Chemical fertilizers and pesticides: role in groundwater
539 contamination, in: Prasad, M.N.V. (Ed.), *Agrochemicals Detection, Treatment and*
540 *Remediation*. Butterworth-Heinemann, pp. 143–159. [https://doi.org/10.1016/B978-0-08-](https://doi.org/10.1016/B978-0-08-103017-2.00006-4)
541 [103017-2.00006-4](https://doi.org/10.1016/B978-0-08-103017-2.00006-4)

542 Swenson, T.L., Jenkins, S., Bowen, B.P., Northen, T.R., 2015. Untargeted soil metabolomics methods
543 for analysis of extractable organic matter. *Soil Biol. Biochem.* 80, 189–198.
544 <https://doi.org/10.1016/j.soilbio.2014.10.007>

545 Tang, F.H.M., Lenzen, M., McBratney, A., Maggi, F., 2021. Risk of pesticide pollution at the global
546 scale. *Nat. Geosci.* 14, 206–210. <https://doi.org/10.1038/s41561-021-00712-5>

547 Tang, X., Zhu, B., Katou, H., 2012. A review of rapid transport of pesticides from sloping farmland to
548 surface waters: Processes and mitigation strategies. *J. Environ. Sci.* 24, 351–361.
549 [https://doi.org/10.1016/S1001-0742\(11\)60753-5](https://doi.org/10.1016/S1001-0742(11)60753-5)

550 Tsugawa, H., Cajka, T., Kind, T., Ma, Y., Higgins, B., Ikeda, K., Kanazawa, M., VanderGheynst, J., Fiehn,
551 O., Arita, M., 2015. MS-DIAL: data-independent MS/MS deconvolution for comprehensive
552 metabolome analysis. *Nat. Methods* 12, 523–526. <https://doi.org/10.1038/nmeth.3393>

553 van Dam, N.M., Bouwmeester, H.J., 2016. Metabolomics in the Rhizosphere: Tapping into
554 Belowground Chemical Communication. *Trends Plant Sci., Special Issue: Unravelling the*
555 *Secrets of the Rhizosphere* 21, 256–265. <https://doi.org/10.1016/j.tplants.2016.01.008>

556 Wang, F., Cao, D., Shi, L., He, S., Li, X., Fang, H., Yu, Y., 2020. Competitive Adsorption and Mobility of
557 Propiconazole and Difenoconazole on Five Different Soils. *Bull. Environ. Contam. Toxicol.*
558 105, 927–933. <https://doi.org/10.1007/s00128-020-03034-1>

559 Wauchope, R.D., Yeh, S., Linders, J.B.H.J., Kloskowski, R., Tanaka, K., Rubin, B., Katayama, A., Kördel,
560 W., Gerstl, Z., Lane, M., Unsworth, J.B., 2002. Pesticide soil sorption parameters: theory,
561 measurement, uses, limitations and reliability. *Pest Manag. Sci.* 58, 419–445.
562 <https://doi.org/10.1002/ps.489>

563 Weber, J.B., Wilkerson, G.G., Reinhardt, C.F., 2004. Calculating pesticide sorption coefficients (Kd)
564 using selected soil properties. *Chemosphere* 55, 157–166.
565 <https://doi.org/10.1016/j.chemosphere.2003.10.049>

566 Werner, D., Garratt, J.A., Pigott, G., 2013. Sorption of 2,4-D and other phenoxy herbicides to soil,
567 organic matter, and minerals. *J. Soils Sediments* 13, 129–139.
568 <https://doi.org/10.1007/s11368-012-0589-7>

569

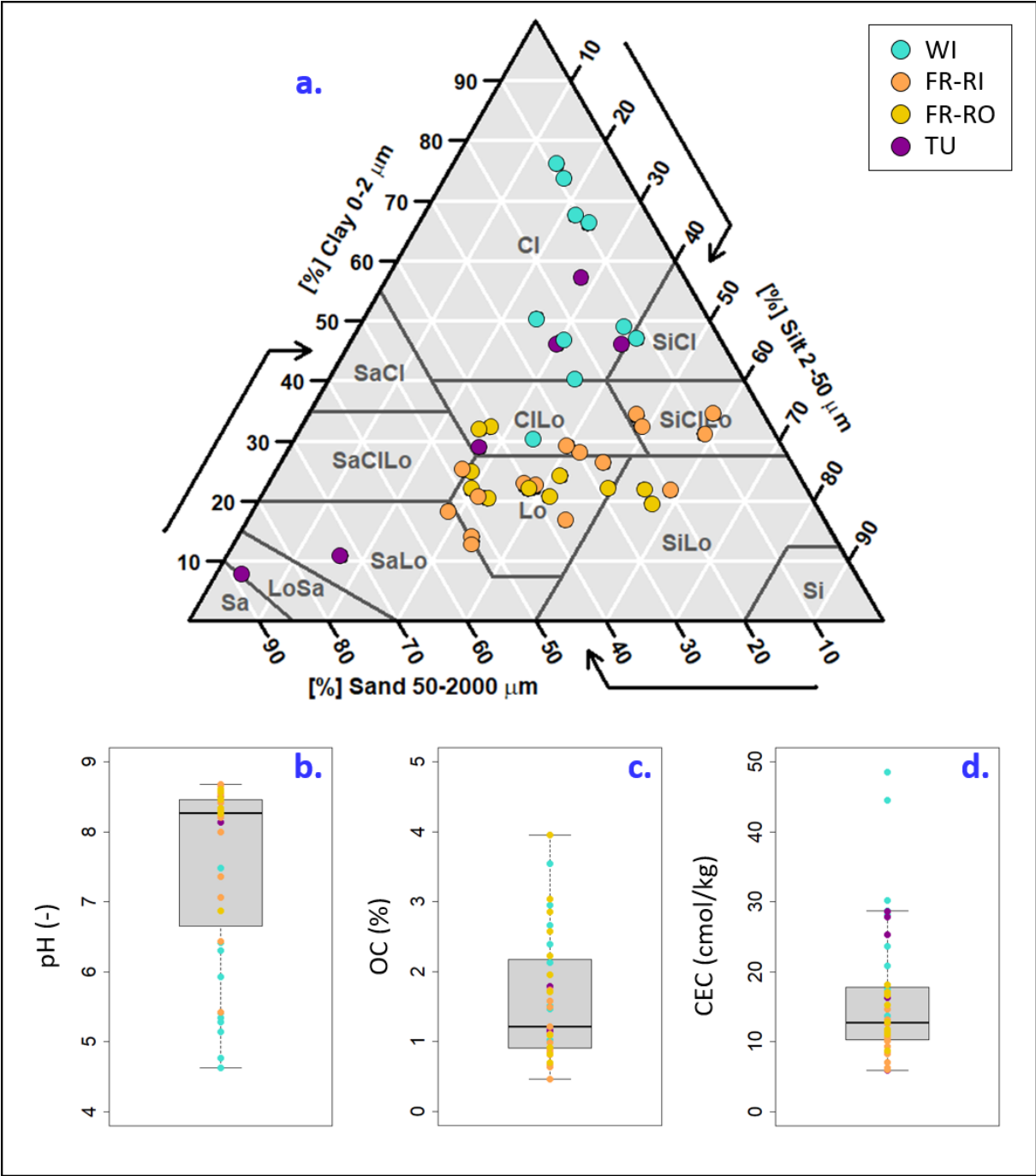


Figure 1: Physico-chemical properties of the soils. This set of 43 soils includes soils sampled in Guadeloupe in the French West Indies (WI), in the Cap Bon Peninsula in Tunisia (TU) and two catchments from southern France (FR-RO and FR-RI). The figure displays the texture range (a.), the pH range (b.), the soil organic fraction range (c.) and the cationic exchange capacity range (d.).

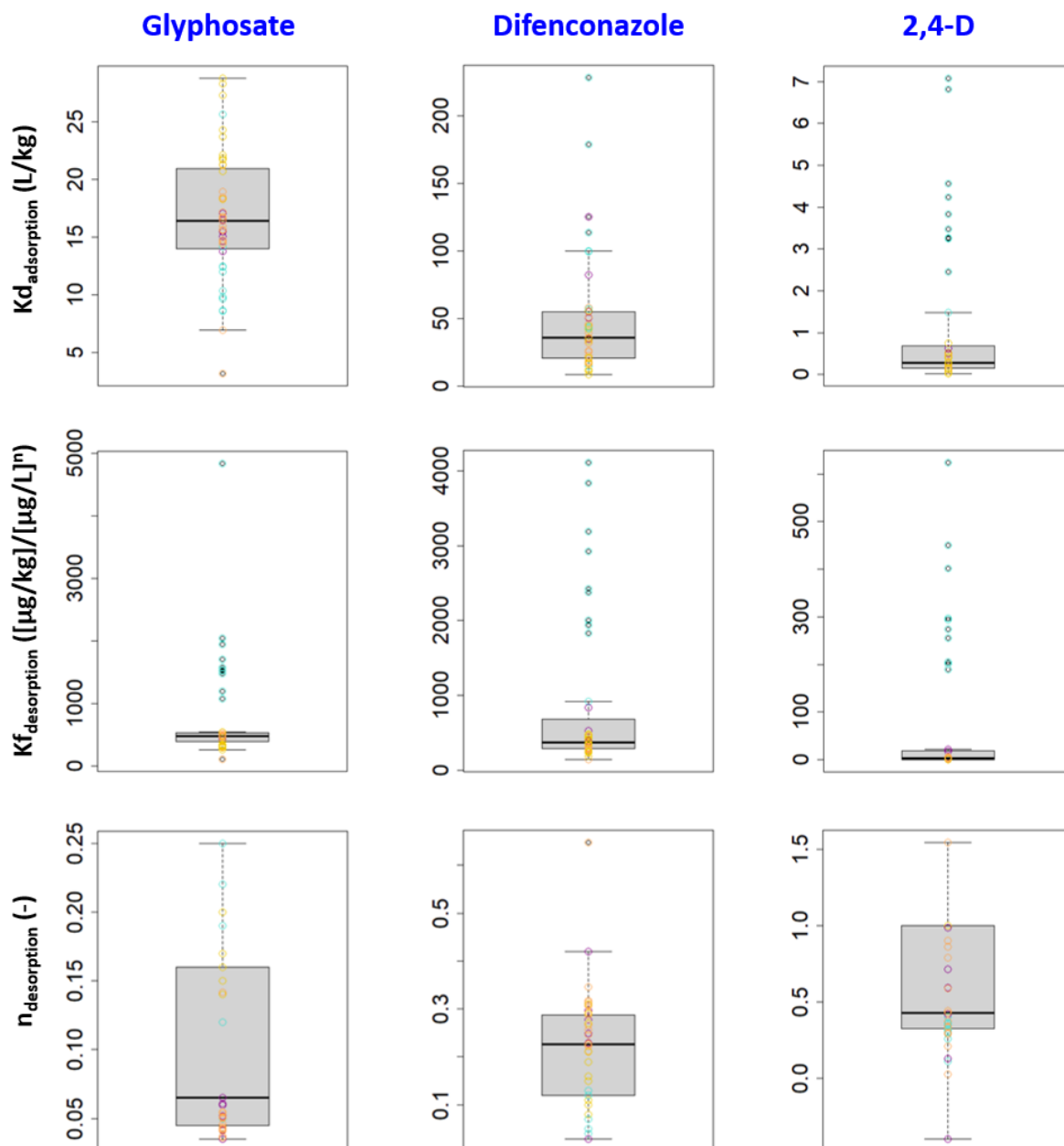


Figure 2: Measured sorption coefficients. The figure shows the distributions of adsorption ($K_{d_{ads}}$) and desorption ($K_{f_{des}}$ & n_{des}) coefficients measured for the WI soils (turquoise dots), the TU soils (violet dots), the FR-RO (gold dots) and FR-RI (orange dots) soils for the pesticides glyphosate, 2,4-D and difenoconazole.



Figure 3: Heatmap of the top 50 discriminant metabolites. The heatmap shows the clustering of the soils according to the relative intensity of the top 50 metabolites identified by an ANOVA analysis. Each lines represent a given metabolite that is further described in Table 1.

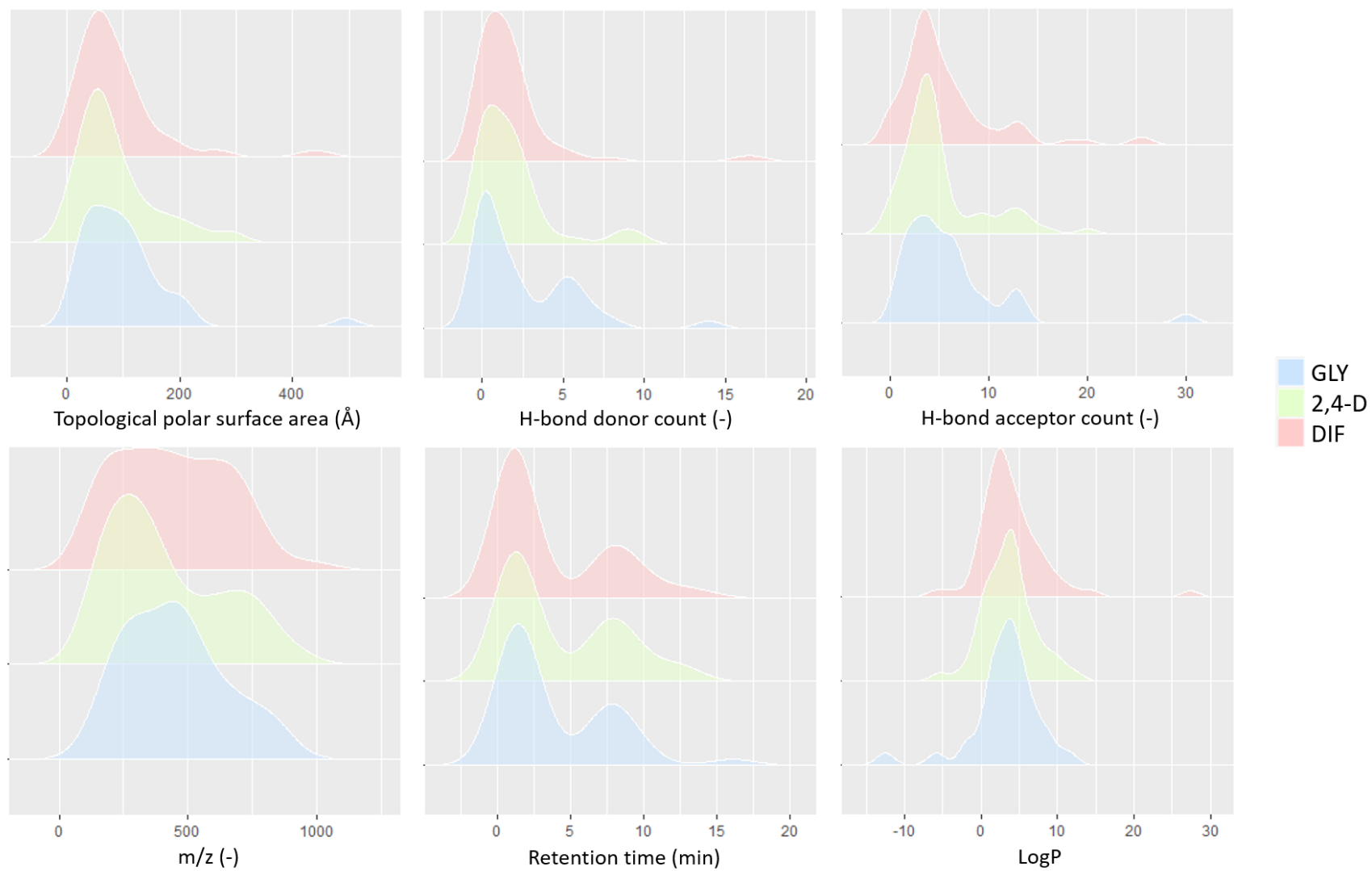


Figure 4: Density functions of six molecular descriptors characterising the most significant features in the PLSR models established to predict the adsorption coefficients (Kd_{ads}) of glyphosate (blue), 2,4-D (green) and difenoconazole (red).

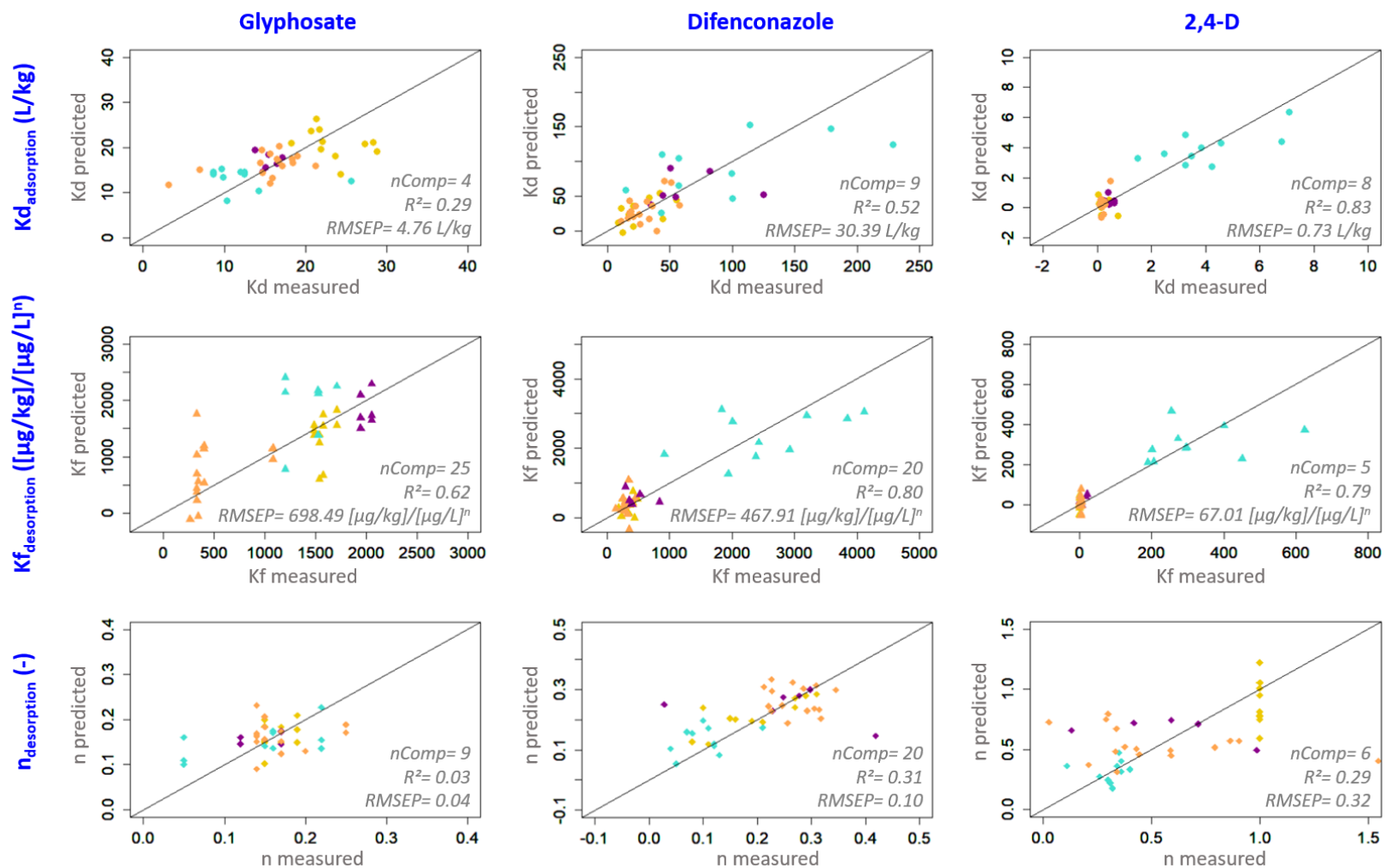


Figure 5: Performance of the PLSR models for the estimation of the sorption coefficients. The plots represent the predicted vs the measured coefficients and their position relative to the 1:1 line (plain diagonal). The performance criteria (R² & RMSEP) as well as the number of components in the PLSR are indicated for each model.

Tables

Table 1: Top 50 features identified by One-way ANOVA discriminating most the molecular profiles of soil organic matter

Compound ID	Average m/z	Average RT (min)	Putative compound (formulation)	Putative level	ΔPPM	Adduct type	Correlation with other ions*
f173	164.03572	8.91	Phthalamic acid (C ₈ H ₇ NO ₃)	2*	-	[M+C ₂ H ₃ N+Na-2H]-	NO
f3922	1018.36053	12.98	Heptadecanoyl CoA (C ₃₈ H ₆₈ N ₇ O ₁₇ P ₃ S)	3	7	[M-H]-	NO
f283	191.03487	7.96	6-Methoxy-7-hydroxycoumarin (C ₁₀ H ₈ O ₄)	2*	-	[M+FA-H]-	NO
f136	159.10287	6.48	2-hydroxy caprylic acid (C ₈ H ₁₆ O ₃)	3	1	[M-H]-	NO
f34	118.03001	6.67	Furo[3,4-b]pyridine (C ₇ H ₅ NO)	3	1	[M-H]-	NO
f1045	305.89166	17.12	2-chloro-4,6-bis(1,1-dichloroethyl)-1,3,5-triazine (C ₇ H ₆ Cl ₅ N ₃)	3	4	[M-H]-	NO
f3624	738.77039	0.95	Phosphoric acid--4-iodophenol (1/3) (C ₁₈ H ₁₈ I ₃ O ₇ P)	3	4	[M-H ₂ O-H]-	NO
f1536	367.01822	5.33	7-Methyl-8-(methylthio)-1-((phenylsulfonyl)oxy)-3,7-dihydro-1H-purine-2,6-dione (C ₁₃ H ₁₂ N ₄ O ₅ S ₂)	3	1	[M-H]-	NO
f451	228.96368	0.96	Diethyl bromomethylphosphonate (C ₅ H ₁₂ BrO ₃ P)	3	1	[M-H]-	YES (m/z 702.87756 & 566.90424 & 498.9166)
f992	301.89148	17.11	4-Bromo-6,6,6-trichloro-3,3-dimethylhex-4-enenitrile	3	1	[M-H]-	NO

			(C8H9BrCl3N)				
f1331	339.02359	8.03	Methanesulfonic acid--[1-(2,4-dichlorophenyl)cyclopentyl]methanol (1/1) (C13H18Cl2O4S)	3	1	[M-H]-	YES (m/z 419.99090)
f677	264.93481	1.01	{{(Methanesulfonyl)methanesulfinyl}methanesulfinyl}methane-SO-thioperoxol (C4H10O5S4)	3	4	[M-H]-	NO
f1715	385.96869	3.31	5'-Hydroxylornoxicam (C13H10ClN3O5S2)	3	2	[M-H]-	NO
f3687	761.76508	0.97	Mercury, (2,4-dibromo-6-(p-bromophenyl)carbonyl)phenoxyphenyl- (C19H12Br3HgNO2)	3	5	[M+K-2H]-	YES (m/z 728.77887 & 598.82501 & 793.76123 & 533.84491)
f736	273.02914	2.40	Simonyellin (C14H10O6)	2*	-	[M-H]-	NO
f865	288.06662	10.12	2-Naphthalenol, 8-(4-amino-2-imino-1,3,5-triazin-1(2H)-yl)-, monohydrochloride (C13H12ClN5O)	3	2	[M-H]-	NO
f180	167.02280	5.25	Uric acid (C5H4N4O3)	2*	-	[2M+FA-H]-	NO
f781	277.10953	9.38	8-(2,3-dihydroxy-3-methylbutyl)-7-methoxychromen-2-one (C15H18O5)	2*	-	[M-H]-	NO
f942	295.22842	13.11	(±)9-HODE (C18H32O3)	3	1	[M-H]-	NO
f974	300.06815	12.42	1-(azepan-1-yl)-3-(3,4-dichlorophenyl)urea (C13H17Cl2N3O)	3	1	[M-H]-	NO
f1512	363.04669	12.26	Quinoxaline, 2-(3-chlorophenyl)-3-[(4-chlorophenyl)methyl]- (C21H14Cl2N2)	3	1	[M-H]-	NO
f1958	417.10638	3.15	2-[(E)-(6-Oxocyclohexa-2,4-dien-1-ylidene)methyl]-N-[4-	3	0	[M-H]-	NO

			(piperidine-1-sulfonyl)phenyl]hydrazine-1-carbothioamide (C ₁₉ H ₂₂ N ₄ O ₃ S ₂)				
f1877	404.10434	1.31	trans-Clovamide (C ₁₈ H ₁₇ NO ₇)	2*	-	[M+C ₂ H ₃ N+Na-2H]-	NO
f675	264.93469	0.98	3-Bromo-7-(trifluoromethyl)imidazo[1,2-b][1,2,4]triazine (C ₆ H ₂ BrF ₃ N ₄)	3	1	[M-H]-	NO
f2996	566.90424	0.98	Trisodium 3,3',3''-phosphinetriyltris(benzene-1-sulphonate) (C ₁₈ H ₁₂ Na ₃ O ₉ PS ₃)	3	7	[M-H]-	YES (m/z 430.92770 & 498.91660)
f959	297.24380	13.52	(9E)-12-hydroxyoctadec-9-enoic acid (C ₁₈ H ₃₄ O ₃)	2*	-	[M-H]-	NO
f2498	484.87045	1.00	3,4-Dibutyl-2,5-diiodothiophene (C ₁₂ H ₁₈ I ₂ S)	3	0	[M+K-2H]-	NO
f1493	359.87125	1.18	Methanesulfonic acid--[1-(2,4-dichlorophenyl)cyclopentyl]methanol (1/1) (C ₁₃ H ₁₈ Cl ₂ O ₄ S)	3	1	[M-H]-	NO
f1952	416.88364	1.00	(2,2-Diiodo-1,1-dimethoxyethyl)benzene1,1-diiodo-2,2-dimethoxy-2-phenylethane (C ₁₀ H ₁₂ I ₂ O ₂)	3	4	[M-H]-	NO
f1711	385.13504	1.40	[3-hydroxy-2-methyl-4-(7-oxofuro[3,2-g]chromen-9-yl)oxybutan-2-yl] (Z)-2-methylbut-2-enoate (C ₂₁ H ₂₂ O ₇)	2*	-	[M-H]-	YES (m/z 371.11993 & 369.14026 & 501.18210)
f2613	501.18167	1.41	NCGC00179938-02 (C ₂₅ H ₂₈ O ₈)	2*	-	[M-H]-	YES (m/z 369.14026 & 355.12506 & 385.13504)
f3677	759.76746	0.88	N,N'-(Hexane-1,6-diyl)didocosanamide	3	4	[M-H]-	NO

			(C50H100N2O2)				
f1826	399.25348	14.52	Anhydro simvastatin (C25H36O4)	3	4	[M-H]-	NO
f402	219.96806	1.29	N-Methyl-2-[(5-sulfanylidene-2,5-dihydro-1,2,4-thiadiazol-3-yl)sulfanyl]acetamide (C5H7N3OS3)	3	0	[M-H]-	NO
f1562	369.14026	1.42	NCGC00380677-01!5,7-dihydroxy-2-(4-hydroxy-3-methoxyphenyl)-6-(3-methylbut-2-enyl)-2,3-dihydrochromen-4-one (C21H22O6)	2*	-	[M-H]-	YES (m/z 355.12506 & 385.13504 & 501.18167)
f3502	695.78937	0.90	-	4	-	-	NO
f3817	843.52698	15.57	Phosphatidylglyceride 20:3-22:6 (C48H77O10P)	2*	-	[M-H]-	NO
f2924	552.85876	1.00	10,11-Dibromoundecyl 2,3-dibromobutanoate (C15H26Br4O2)	3	1	[M-H]-	YES (m/z 620.84650 & 484.87045)
f353	209.93593	11.74	(2-Bromo-5-fluorophenoxy)acetonitrile (C8H5BrFNO)	3	2	[M-H2O-H]-	NO
f27	114.38640	2.54	-	4	-	-	NO
f70	135.04543	6.07	Caffeic acid (C9H8O4)	2*	-	[M-H]-	NO
f1299	332.92239	1.00	4-(4-Chlorobenzene-1-sulfonyl)-3-methylthiophene-2-carbonyl chloride (C12H8Cl2O3S2)	3	0	[M-H]-	NO
f2516	486.03067	1.28	9-Bromo-3,3-bis(4-fluorophenyl)-3,11-dihydropyrano[3,2-a]carbazole (C27H16BrF2NO)	3	0	[M-H]-	NO
f1124	313.23865	13.17	9,10-dihydroxy-12-octadecenoic acid (C18H34O4)	3	0	[M-H]-	NO
f1959	417.10754	4.43	1,3-dioxo-2-(oxolan-2-ylmethyl)-N-[4-	3	1	[M-H]-	NO

			(trifluoromethyl)phenyl]isoindole-5-carboxamide (C ₂₁ H ₁₇ F ₃ N ₂ O ₄)				
f2106	434.87146	1.16	5,5-bis(2-iodoethyl)pyrimidine-2,4,6(1h,3h,5h)-trione (C ₈ H ₁₀ I ₂ N ₂ O ₃)	3	1	[M-H]-	YES (m/z 304.91415)
f2539	489.12576	10.85	3-(5-{{1-Butyl-5-cyano-4-methyl-2-(morpholin-4-yl)-6-oxo-1,6-dihydropyridin-3-yl}methylidene}-4-oxo-2-sulfanylidene-1,3-thiazolidin-3-yl)propanoic acid (C ₂₂ H ₂₆ N ₄ O ₅ S ₂)	3	2	[M-H]-	NO
f83	144.04565	7.69	8-Hydroxyquinoline (C ₉ H ₇ NO)	2*	-	[M-H]-	NO
f2404	471.07892	1.45	Propanamide, N-[2-[(2-bromo-6-cyano-4-nitrophenyl)azo]-5-(diethylamino)phenyl]- (C ₂₀ H ₂₁ BrN ₆ O ₃)	3	1	[M-H]-	NO
f868	288.93649	1.06	2-bromo-5-(trifluoro methyl)phenylhydrazine hydrochloride (C ₇ H ₇ BrClF ₃ N ₂)	3	1	[M-H]-	YES (m/z 456.86319)
f918	293.17630	11.45	Embelin (C ₁₇ H ₂₆ O ₄)	2*	-	[M-H]-	NO

* Compounds annotated with MS-DIAL other annotations were performed with METLIN (see section 2.5)